



Resting state fMRI based multilayer network configuration in patients with schizophrenia

George Gifford^{a,*}, Nicolas Crossley^{a,b}, Matthew J Kempton^a, Sarah Morgan^{c,d}, Paola Dazzan^a, Jonathan Young^a, Philip McGuire^a

^a Department of Psychosis Studies, Institute of Psychiatry, Psychology and Neuroscience, King's College London, De Crespigny Park, London SE5 8AF, UK

^b Department of Psychiatry, School of Medicine, Pontificia Universidad Católica de Chile, Diagonal Paraguay 362, Santiago 8330077, Chile

^c Department of Psychiatry, University of Cambridge, Cambridge CB2 0SZ, UK

^d The Alan Turing Institute, London NW1 2DB, UK

ARTICLE INFO

Keywords:

Resting State fMRI
Modularity
Dynamic functional connectivity
Multilayer community detection
Flexibility
Network switching
Schizophrenia
Module allegiance
Transition matrix

ABSTRACT

Novel methods for measuring large-scale dynamic brain organisation are needed to provide new biomarkers of schizophrenia. Using a method for modelling dynamic modular organisation (Mucha et al., 2010), evidence suggests higher ‘flexibility’ (switching between multilayer network communities) to be a feature of schizophrenia (Braun et al., 2016). The current study compared flexibility between 55 patients with schizophrenia and 72 controls (the COBRE Dataset). In addition, novel methods of ‘between resting state network synchronisation’ (BRSNS) and the probability of transition from one community to another were used to further describe group differences in dynamic community structure. There was significantly higher schizophrenia group flexibility scores in cerebellar ($F(1124) = 9.33$, $p(\text{FDR}) = 0.017$), subcortical ($F(1124) = 13.14$, $p(\text{FDR}) = 0.005$), and fronto-parietal task control ($F(1124) = 7.19$, $p(\text{FDR}) = 0.033$) resting state networks (RSNs), as well as in the left thalamus (MNI XYZ: -2, -13, 12; $F(1, 124) = 17.1$, $p(\text{FDR}) < 0.001$) and the right crus I (MNI XYZ: 35, -67, -34; $F(1, 124) = 19.65$, $p(\text{FDR}) < 0.001$). Flexibility in the left thalamus reflected transitions between communities covering default mode and sensory-somatomotor RSNs. BRSNS scores suggested altered dynamic inter-RSN modular configuration in schizophrenia. This study suggests less stable community structure in a schizophrenia group at an RSN and node level and provides novel methods of exploring dynamic community structure. Mediation of group differences by mean time window correlation did however suggest flexibility to be no better as a schizophrenia biomarker than simpler measures and a range of methodological choices affected results.

Acronyms

BRSNS – Between Resting State Network Synchronisation
ORSNS – Out of Resting State Network Synchronisation
RSN – Resting State Network

1. Introduction

Schizophrenia has been conceptualised as a disorder of dysconnectivity (Pettersson-Yeo et al., 2011), which is supported by meta-analyses of structural (Ellison-Wright and Bullmore, 2009) and functional imaging studies (Dong et al., 2017; O'Neill et al., 2018). Resting state functional connectivity studies have implicated altered connectivity of the default mode network (Dong et al., 2017; Kühn and Gallinat, 2011; O'Neill et al., 2018), cortical-subcortical dysconnectivity

(Damaraju et al., 2014; Woodward et al., 2012), and abnormal whole brain network topology measures such as lower connectedness of hubs (Lynall et al., 2010) and lower network modularity (Alexander-Bloch et al., 2010; Lerman-Sinkoff and Barch, 2016; Yu et al., 2012).

Functional connectivity alterations in schizophrenia are suggested to be both complex (Dong et al., 2017) and transitory, with intermittent states of dysconnectivity apparent over the course of a scan (Damaraju et al., 2014; Du et al., 2017; Rashid et al., 2016, 2014). The difficulties of characterising functional connectivity alterations that are both complex and time varying highlights the need for novel methods that can simultaneously take into account large-scale brain organisation and dynamics. A development in the ‘dynamic network neuroscience’ field has been the application of multilayer community detection, a method for modelling time-varying community structure across the course of a scan (Mucha et al., 2010).

* Corresponding author.

E-mail address: george.gifford@kcl.ac.uk (G. Gifford).

<https://doi.org/10.1016/j.nicl.2020.102169>

Received 13 September 2019; Received in revised form 18 December 2019; Accepted 10 January 2020

Available online 11 January 2020

2213-1582/ Crown Copyright © 2020 Published by Elsevier Inc. This is an open access article under the CC BY-NC-ND license (<http://creativecommons.org/licenses/by-nc-nd/4.0/>).

Multilayer community detection has been used to explore the “flexibility” (Bassett et al., 2011) or “node switching” (Pedersen et al., 2018; Telesford et al., 2017) of brain areas. Multilayer community detection describes the clustering of highly connection regions, allowing community structure to change over time. Flexibility can be seen as a generic measure of dynamic community structure and is not specifically related to concepts such as cognitive flexibility. For instance, flexibility has been related to diverse aspects of cognition, such as motor learning (Bassett et al., 2011), recognition memory (Telesford et al., 2016), attention (Shine et al., 2016; Telesford et al., 2016), working memory (Braun et al., 2016), executive function (Braun et al., 2015), cognitive inhibition, cognitive flexibility, processing speed, and planning (Pedersen et al., 2018). It has also been associated with fatigue, surprise and positive affect (Betz et al., 2017), and depression (Zheng et al., 2018).

One study to date has explored flexibility in schizophrenia, suggesting whole brain flexibility to be higher in patients with schizophrenia during a working memory task (Braun et al., 2016). The current study builds on this research by comparing flexibility scores between a patient group with schizophrenia and a healthy control group during a resting state fMRI scan. In addition, the current study used two novel methods in an attempt to further characterise group differences in dynamic modular configuration. One approach used the “module allegiance matrix” (Bassett et al., 2015) in order to measure the level of synchronisation between brain areas and between previously defined resting state networks (RSNs) (Power et al., 2011). A second method used K-means clustering and transition matrices in order to make group comparisons of the probability of transition between communities. The aim of this study was to build on the previous finding of Braun et al. (2016) and to provide novel methods of exploring dynamic functional connectivity in schizophrenia.

1.1. Hypotheses

The main hypothesis was that when assessed in the resting state, flexibility scores would be higher in patients with schizophrenia than controls. We tested this hypothesis at a whole brain, RSN, and node level. Multilayer community assignment was further described in an exploratory analysis using two novel measures, between resting state network synchronisation (BRSNS) and the probability of transition between communities. In order to validate these methods and to provide a normative model, flexibility and module allegiance was first tested in the control sample alone.

2. Methods

2.1. Participants

The COBRE dataset has 72 patients with schizophrenia and 75 healthy controls. Participants underwent a 5 minute resting state scan (TR = 2s, TE = 29 ms, 150 volumes, matrix size = 64×64 , 32 slices, voxel size = $3 \times 3 \times 4$ mm³). Two controls and 19 patients were removed during preprocessing (see below), and two participants withdrew their data, leaving data from 72 controls and 55 patients for analysis. Group characteristics are described in Table 1.

2.2. Preprocessing

Preprocessing followed the same steps as in Patel et al. (2014) using AFNI version 17.2.17 (Cox, 1996) and FSL version 5.0.11 (Jenkinson et al., 2012). Briefly this involved slice timing correction, rigid-body head movement realignment to the first volume, co-registration to structural image using a gray matter mask, transformation to MNI space, spatial smoothing with a 6 mm FWHM, wavelet despiking using the BrainWavelet Toolbox with default settings (www.brainwavelet.org), regression of 6 movement parameters (x, y, z,

Table 1

Demographics of the COBRE dataset used in this study, including gender, age (mean and standard deviation), and handedness. Chi-squared / Mann-Whitney U / Fischer's Exact tests were used to judge whether group differences were problematic. For the patient group Positive and Negative Syndrome Scale (PANSS) scores are given, as well as medication (olanzapine equivalent dose in mg), age of onset of psychotic symptoms, and duration of psychotic illness in years.

	Patients (N = 55)	Controls (N = 72)	Significance Test	P
Gender			$\chi^2 (1) = 3.23$	0.072
Male (%)	46.00 (83.64)	49.00 (68.06)		
Female (%)	9.00 (16.36)	23.00 (31.94)		
Mean Age (SD)	36.11 (13.59)	35.86 (11.67)	T (106.32) = -0.11	0.914
Handedness			Fischer's Exact Test	0.012
Right (%)	46.00 (83.64)	69.00 (85.83)		
Left (%)	8.00 (14.55)	1.00 (1.39)		
Both (%)	1.00 (1.82)	2.00 (2.78)		
PANSS				
Positive	14.82 (4.75)			
Negative	14.49 (5.13)			
General	29.33 (8.28)			
Olanzapine	10.65 (6.24)			
Equivalent (mg)				
Age of Onset (years)	20.85 (7.78)			
Duration of Illness (years)	15.00 (12.53)			

pitch, roll, and yaw) and CSF based confounding signal. A band-pass filter of $0.08 < f < 0.15$ Hz was applied, which is the same frequency band studied in a previous investigation of flexibility in schizophrenia (Braun et al., 2016).

Although the Wavelet Despiking algorithm is a robust movement correction procedure (Patel et al., 2014) there was a significant difference in median mean spike percentage (a measure of movement related noise) between the two groups (U = 1598, p < 0.001). Participants with a mean spike percentage > 7.5% were excluded from the analysis, however there was still a higher median mean spike percentage in the patient group (U = 1477, p = 0.014). As a result, mean spike percentage was included as a covariate in the group comparisons.

Resting state scans were parcellated using the Power et al. (2011) atlas (5mm spheres around suggested coordinates). This atlas was chosen as it has pre-defined allocations of nodes into RSNs. The Power et al. (2011) atlas has 12 RSNs: default mode, cerebellar, cingulo-opercular task control, sensory-somatomotor hand / mouth, sub-cortical, fronto-parietal task control, visual, memory retrieval, salience, dorsal attention, ventral attention, and auditory. In the current study the two sensory-somatomotor networks were combined. To confirm results main group comparisons of flexibility were repeated using the Gordon et al. (2016) atlas, which contains a similar set of 11 RSNs, with the omission of the cerebellar, subcortical, and memory retrieval networks, and the addition of the retrosplenial-temporal and cingulo-parietal RSNs. These two atlases were chosen as they have pre-defined allocations of nodes into RSNs.

Areas of signal drop out were defined as those with a mean time-series signal intensity z score (across nodes) less than or equal to 1.64 in any subject, corresponding to outliers > 95th percentile or < 5th percentile. These nodes were removed from the analysis, leaving 207 regions in the Power et al. (2011) parcellation and 268 in the Gordon et al. (2016) parcellation. Areas of signal loss were mostly in ventral prefrontal and temporal areas, which is a common issue in MRI imaging (Deichmann et al., 2003).

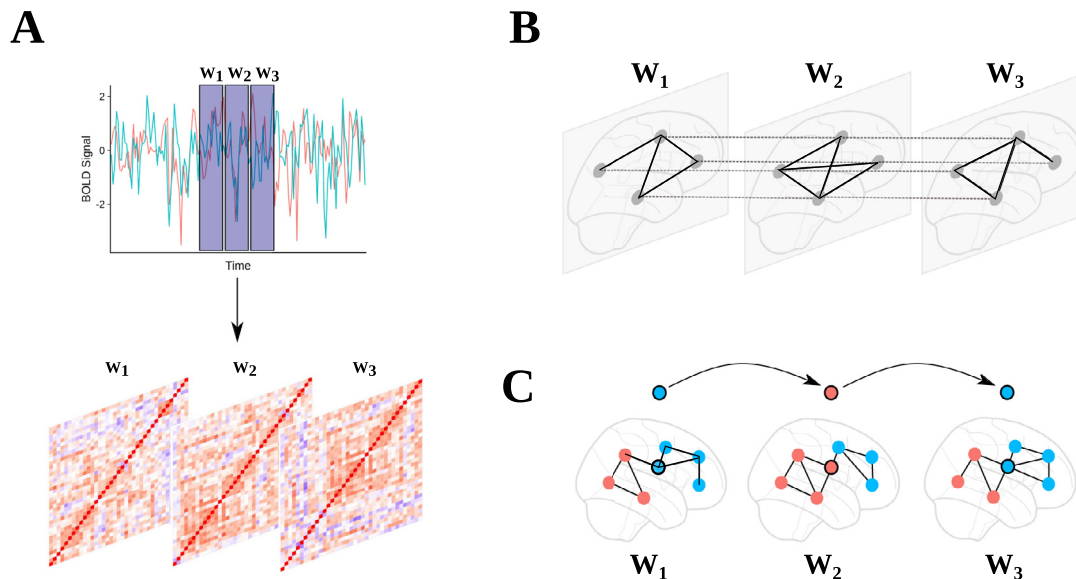


Fig. 1. (A) Blood oxygen level-dependent (BOLD) signals from 207 regions (Power et al. (2011); ROIs with low SNR areas removed) were extracted and non-overlapping windowed segments were used to create a sequence of node by node correlation matrices. (B) Thresholded correlation matrices were used to create a multilayer network with inter-layer edges connecting nodes at the same location in each windowed graph. (C) A multilayer community detection algorithm was used (Mucha et al., 2010) to give community assignments at each window. Flexibility was computed as the mean number of times a node changed community assignment.

2.3. Sliding time windows

Time-series data were split into a consecutive series of non-overlapping windows. Similar to Braun et al. (2016) scans were cut into 30 s / 15 TR segments. Additionally, flexibility results were repeated with 25 TRs (50 s) and 30 TRs (60 s) window sizes, in order to report whether window size affected results. These window sizes were chosen so that the total number of volumes (150) was divisible by each window length and because it has been suggested that 30–60 s time windows are reasonable in studying fMRI based dynamic functional connectivity (Leonardi and Van De Ville, 2015) and such window sizes have typically been used in dynamic functional connectivity studies (Allen et al., 2014; Chang and Glover, 2010; Hutchison et al., 2013; Sakoğlu et al., 2010; Shirer et al., 2012; Gonzalez-Castillo et al., 2013). It has been suggested also that the minimum window size that can be used in a dynamic functional connectivity study is $1/f_{min}$, where f_{min} is the minimum frequency included (Leonardi and Van De Ville, 2015). In the present study this would allow for a window size of 12.5 s ($1/0.08 = 12.5$). However, window sizes below 30 s appeared to have low variance of flexibility across participants and across nodes (supplementary materials Section 1).

Windowed correlation matrices were proportionally thresholded at 10% to give a series of weighted adjacency matrices. Adjacency matrices in sequence were used as ordered layers in the multilayer network. Additionally, the analysis was repeated at 5 and 15% thresholds, as well as over a range of parameters specific to the multilayer community detection algorithm: γ (0.9, 1, 1.1) and ω (0.5, 0.75, 1) (Pedersen et al., 2018). The parameter γ controls the size and therefore number of communities within layers of the network (larger $\gamma =$ more communities). The parameter ω in the current study controls the number of communities found across layers (larger $\omega =$ less communities) (Bassett et al., 2013). An exploration of how these parameters affected flexibility and group differences is shown in the supplementary materials Section 1.

2.4. Multilayer community detection

Communities describe groups of nodes more strongly connected to each other than to nodes outside of their community, as compared to a null model representing what would be expected in a network of similar

size and density with randomly distributed connections (Newman, 2006). Modularity describes a formal measurement of this (Newman and Girvan, 2004), which can be used in iterative processes of finding a partition of a network with an optimal set of community assignments. In the current study the GenLouvain community detection algorithm was used (Jutla et al., 2011; Mucha et al., 2010), which involves the following modularity measurement that is formulated to work on multilayer networks:

$$Q = \frac{1}{2\mu} \sum_{ijlr} [(A_{ijl} - \gamma_1 P_{ijl})\delta_{lr} + \delta_{ij}\omega_{jlr}]\delta(g_{il}, g_{jr})$$

Here μ is the total edge weight of the network, A_{ijl} is the adjacency matrix between nodes i and j at layer l . P_{ijl} describes the matrix of expected weights under the null model. The structural resolution parameter γ_1 sets the weight of intralayer edges, and the temporal ω_{jlr} resolution parameter sets the weight of inter layer edges (here $\gamma_1 = \omega_{jlr} = 1$). g refers to community assignments: g_{il} and g_{jr} are the community assignments of node i in layer l , and node j in layer r (respectively). δ describes the Kronecker delta, which for $\delta(g_{il}, g_{jr})$ is 1 if $il = jr$, and 0 if $il \neq jr$ (Bassett, Porter, et al., 2013)

In the current study the GenLouvain community detection algorithm was used on each participant's sequence of weighted adjacency matrices (node \times node \times layer). Here, the network was treated as ordinal, with interlayer links between sequential layers for nodes at the same position. This was a similar implementation used in previous studies (Bassett et al., 2011; Braun et al., 2016; Pedersen et al., 2018; Telesford et al., 2016) (Fig. 1).

2.5. Module allegiance and between / out of RSN synchronisation

In order to measure the dynamic reorganisation of communities between RSNs the concept of a “module allegiance matrix” (Bassett et al., 2015; Zheng et al., 2018) was used. This concept has also been termed the “temporal co-occurrence matrix” in a previous study (Chen et al., 2016). The benefit of the module allegiance matrix is that it allows for the level of synchronisation between specific nodes or RSNs to be measured. To create each participant's module allegiance matrix a node \times node matrix was formed with each element giving the proportion of times a node shared a community with another node over the

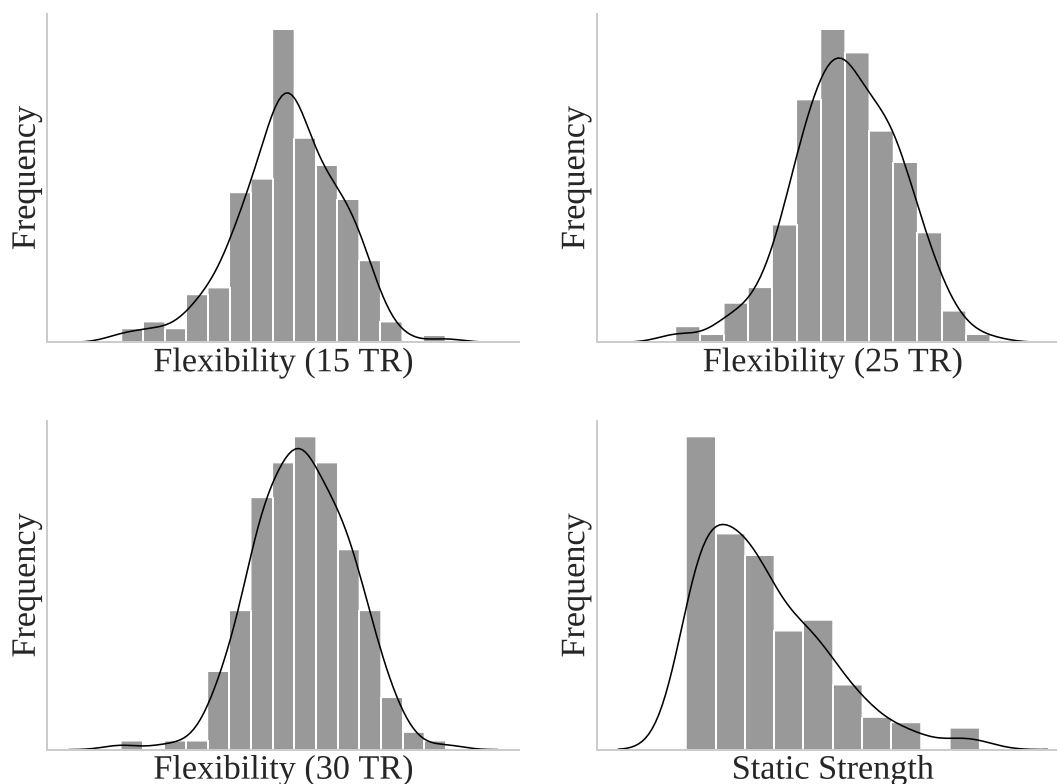


Fig. 2. Distribution of Flexibility (for 15, 25, and 30 TRs) and static (whole time series) strength (weighted degree) for all nodes within controls.

course of the scan.

Mean module allegiance between RSNs was found in order to give a measure of synchronisation between pairs of RSNs. We refer to this measure as ‘between RSN synchronisation’ (BRSNS). To provide a summary measure of how often RSNs coupled with nodes outside of their network, the mean of all out of RSN module allegiance values for each RSN was taken. For simplicity we refer to this measure as ‘out of RSN synchronisation’ (ORSNS). This is a similar concept to “temporal flexibility” proposed by Chen et al. (2016). ORSNS was measured in controls in order to validate the module allegiance procedure, by comparing relative levels with suggested ‘processing / control’ profiles of RSNs (Power et al., 2011), which are described based on profiles of inter and intra RSN connectivity.

2.6. Transition matrices

A transition matrix containing the probability of transition from one community to another was formed for each participant. Group differences were then tested using permutation tests (two tailed; 5000 permutations of group assignments). Transition matrices were treated as undirected by averaging inward and outward transition probabilities.

K means clustering was used (Scikit-Learn: Pedregosa et al., 2011) in order to label the communities found in each participant into a set of standard communities shared across subjects. This approach is commonly used with dynamic functional connectivity as it provides a way to standardise participant’s sliding time windows into a set of group meta-states (Allen et al., 2014; Damaraju et al., 2014; Rashid et al., 2014; Shakil et al., 2016). Every community from every participant was entered into the k means algorithm, the feature space being a vector of probability of node assignment for all nodes (207 features). A full description of the k means procedure is given in the supplementary materials Section 2. Each cluster was equally represented in patient and controls groups (supplementary materials Table 2.1).

2.7. Confounding factors

Group characteristics suggested a significant difference in the proportions of left and right handed participants (Fischer’s Exact Test, $p = 0.012$). As some cell counts would be too small to enter as a covariate in a logistic regression the results were instead repeated including only right handed participants. In addition, the analysis was repeated using overlapping windows (in steps of 1 TR), as previous studies have used both overlapping / non overlapping windows (Bassett et al., 2011; Braun et al., 2016; Pedersen et al., 2018; Telesford et al., 2016).

It is also the case that complex measures such as flexibility may be explained by simpler network characteristics. The current study tested whether the mean number of communities in time windows and the mean of time windowed correlation matrices were mediators in the relationship between group assignment and flexibility.

2.8. Ethics statement

The COBRE (The Centre for Biomedical Research Excellence) dataset was obtained through the International Neuroimaging Data-sharing Initiative (http://fcon_1000.projects.nitrc.org/indi/retro/cobre.html). This was originally released under Creative Commons – Attribution Non-Commercial. Written informed consent was obtained for all participants.

2.9. Code availability

In order to aid reproducibility and transparency, tailor made scripts used in this study have been made available (https://github.com/george-gifford/COBRE_multilayer_community). Statistical analysis was performed using R version 3.5.1. The current study used a Matlab version 9.2.0. when implementing the GenLouvain multilayer community detection algorithm, which is currently available from (netwiki.amath.unc.edu/GenLouvain/GenLouvain) (Jutla et al., 2011).

3. Results

3.1. Flexibility in controls

We first investigated whether flexibility correlated with static strength (weighted degree). In each of the 15 TR ($r_s = 0.55$, $p < 0.001$), 25 TR ($r_s = 0.42$, $p < 0.001$), and 30 TR windows ($r_s = 0.42$, $p < 0.001$) strength was significantly correlated with flexibility. This suggests that higher degree nodes typically had higher flexibility. The distribution of flexibility values across nodes for all window sizes indicated a normal distribution, and static strength followed a power law distribution with a minority of high strength nodes (Fig. 2).

3.2. Most / least flexible nodes in controls

The nodes with the highest flexibility scores across window sizes were located in the bilateral precentral gyrus, right post-central gyrus, left supplementary motor cortex, lateral occipital cortex, right middle temporal gyrus, right supramarginal gyrus, and the right precuneus cortex. Nodes with the lowest flexibility scores were in the right middle frontal gyrus, right parahippocampal gyrus, bilateral precentral gyrus, right superior frontal gyrus, left brain stem, right anterior cingulate gyrus, left para-cingulate gyrus, left posterior cingulate gyrus, left thalamus, and right posterior cingulate gyrus (Fig. 3, also see supplementary materials Section 3). Taking the mean flexibility scores of nodes within each RSN the default mode consistently showed the lowest flexibility scores across window sizes. The auditory, dorsal attention, and ventral attention RSNs consistently showed the highest flexibility scores.

3.3. Module allegiance in controls

A node x node matrix of mean module allegiance values across controls showed higher module allegiance of nodes within each RSN, particularly within visual, default mode, and sensory-somatomotor networks (Fig. 4). ORSNS for each RSN was highest for the ventral attention and cerebellar RSNs and lowest for the sensory-somatomotor, default mode, and visual RSNs (Fig. 4). This was consistent over window sizes (supplementary materials Section 4). The highest BRSNS score was between the default mode and memory retrieval, the salience and subcortical, and subcortical and cerebellar networks. The lowest BRSNS score was between the memory retrieval and auditory, dorsal attention and subcortical, and subcortical and sensory-somatomotor networks. Results for 25 and 30 TR windows are shown in the supplementary materials Section 4.

3.4. Group comparisons – Whole brain

Whole brain mean flexibility values were compared between patient and control groups. This was done whilst controlling for mean spike percentage using Analysis of Covariance (ANCOVA) (Table 2). Group distributions of flexibility are shown in Fig. 5. Flexibility was not significantly different between patients and controls at the 15, 25, and 30 TR window sizes. Bootstrapped confidence intervals of beta values suggested a trend for significantly higher flexibility in the schizophrenia patient group (Table 2). Results using the Gordon et al. (2016) parcellation are shown in supplementary materials Section 5.1.

3.5. Group comparisons – Resting state networks

RSN mean flexibility values were compared between the patient and control groups. This was done whilst controlling for spike percentage

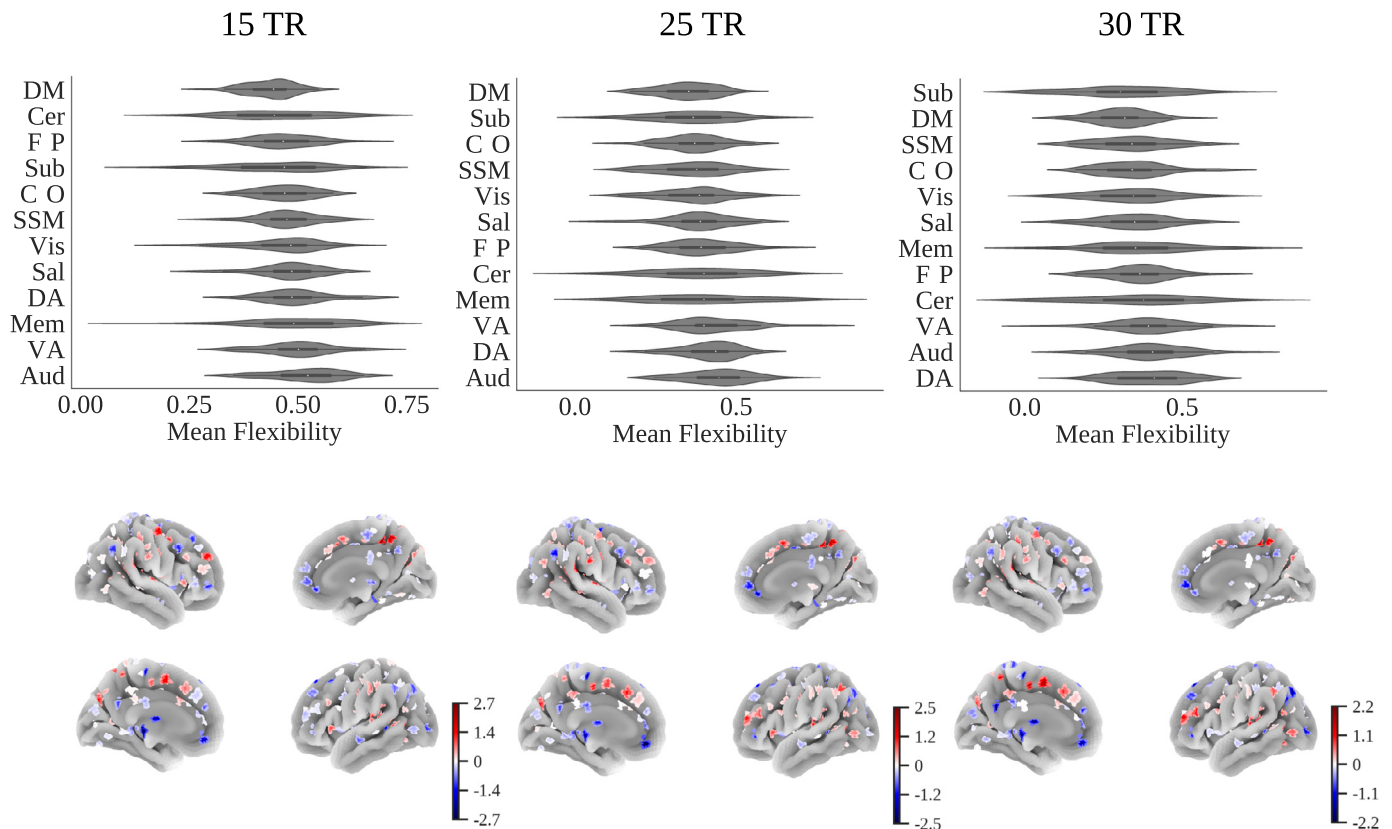


Fig. 3. Upper: Violin plots of mean flexibility scores averaged within each resting state network for each participant for 15, 25, and 30 TR windows. Lower: Mean flexibility (zscore) across all controls for 15, 25, and 30 TR thresholds projected onto a cortical surface.

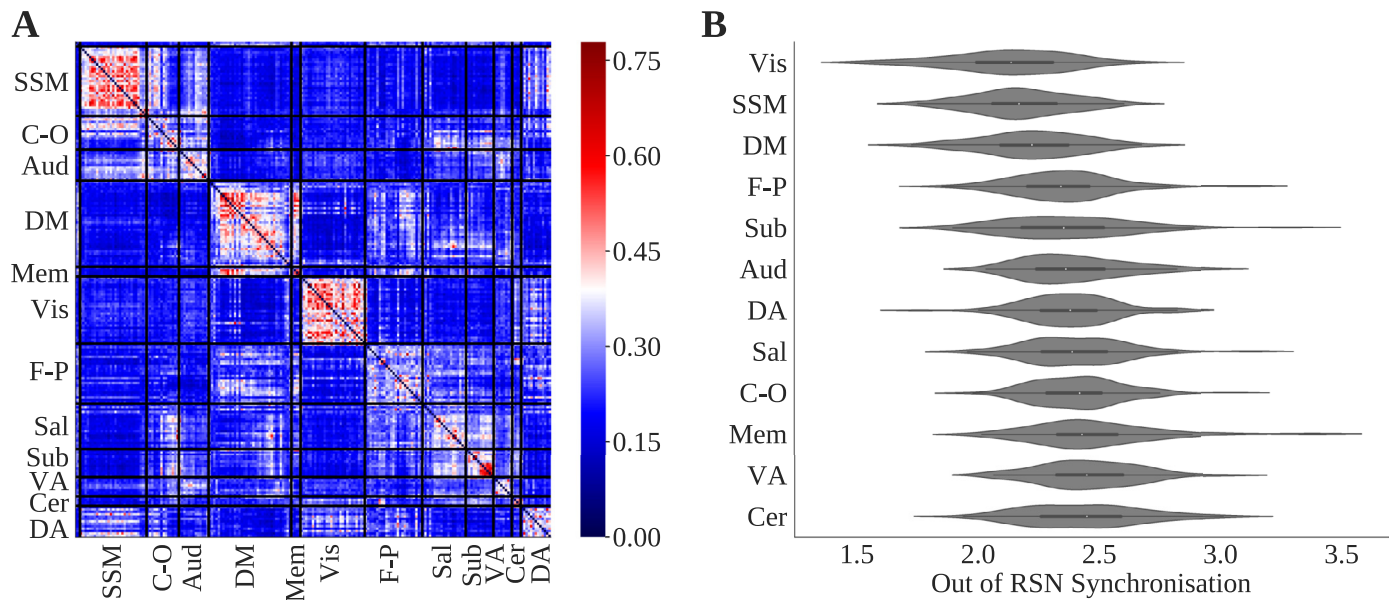


Fig. 4. (A) Node x node module allegiance matrix. Bar shows proportion of times nodes share the same community. (B) Violin plot of resting state network (RSN) out of network synchronisation (ORSNS) for each RSN. Both plots show results for 15 TR windows.

Table 2

Group mean and standard deviation whole brain flexibility for 15, 25, and 30 TR window sizes. F and P values are displayed. CI: Bootstrapped (5000 permutations) 95% confidence intervals of Beta values.

Window size	Patient Mean	(SD)	Control Mean	(SD)	F, DOF (1124)	P	B	Bootstrapped 95% CI	
15 TR	0.47	0.03	0.46	0.04	2.82	0.095	0.005	0.000	0.011
25 TR	0.38	0.05	0.38	0.05	0.95	0.331	0.004	-0.005	0.013
30 TR	0.35	0.07	0.34	0.05	1.01	0.317	0.005	-0.005	0.016

using an ANCOVA. All results were non-significant (see supplementary materials Section 6 for full results) apart from in the cerebellar ($F(1124) = 9.33$, $p(\text{FDR}) = 0.017$), subcortical ($F(1124) = 13.14$, $p(\text{FDR}) = 0.005$), and fronto-parietal task control networks ($F(1124) = 7.19$, $p(\text{FDR}) = 0.033$) when using 15 TR windows. Bar charts of RSN flexibility values are shown in Fig. 5. Results using the Gordon et al. (2016) parcellation are shown in supplementary materials Section 5.2.

3.6. Group comparisons – All nodes

Group comparisons of flexibility were made at a node level between patients and controls. When controlling for multiple comparisons (FDR) two regions were significantly different in terms of flexibility for the 15 TR window size: a node in the left thalamus (MNI XYZ: -2, -13, 12; $F(1, 124) = 17.1$, $p(\text{FDR}) < 0.001$) and the right crus I, which is part of the cerebellum (MNI XYZ: 35, -67, -34; $F(1, 124) = 19.65$, $p(\text{FDR}) < 0.001$). For the Gordon et al. (2016) parcellation likewise no regions were found to be significant at the 15 TR window size. When using 25 TR windows a node in the right insula was found to be more flexibility in patients with schizophrenia (MNI XYZ: 39.6, 10.4, -1.6; $F(1124) = 15.04$, $p(\text{FDR}) < 0.001$).

3.7. Correlation with PANSS scores, age of onset, medication, and duration of illness

Within the patient group, whole brain flexibility as well as flexibility in brain areas / RSNs that were significantly different between groups was compared with positive and negative PANSS scores, age of onset of psychotic symptoms, and duration of psychosis. Positive PANSS scores were weakly significantly negatively correlated with whole brain

flexibility (15 TR) ($R_s = -0.27$, $p = 0.042$) and duration of illness was moderately significantly negatively correlated with flexibility within the subcortical RSN ($R_s = -0.30$, $p = 0.025$). No correlations were significant after correcting for multiple comparisons. Full results are shown in Table 3. Results using the Gordon et al. (2016) parcellation shown in supplementary materials Section 6.

3.8. Group comparisons – Module allegiance

The aim of using module allegiance was to further describe group differences in the dynamic configuration of communities in an exploratory manner. To do so independent group t tests were performed for group differences of BRSNS scores for all RSN pairs (Table 4). An FDR correction was applied to p values across 66 tests. This was done for 15 TR windows only as there were no significant differences in flexibility for the 25 and 30 TR windows at the RSN level.

There were also significant correlations between BRSNS scores and positive PANSS symptom scores for sensory somatomotor / salience ($r = -0.33$, $p = 0.014$) and salience / subcortical RSNs ($r = -0.27$, $p = 0.045$), and negative PANSS symptom scores for auditory / cerebellar RSNs ($r = 0.30$, $p = 0.025$). No BRSNS scores were correlated with illness duration, age of onset of psychotic symptoms or medication use. These correlations were not significant when controlling for multiple comparisons (Fig. 6).

3.9. Transition matrices

Using communities tokenised by a K means clustering procedure, matrices of the probability of transition from one community to another were created for all nodes. This was done at the whole brain level (mean transition matrices across nodes) and for the node located in the

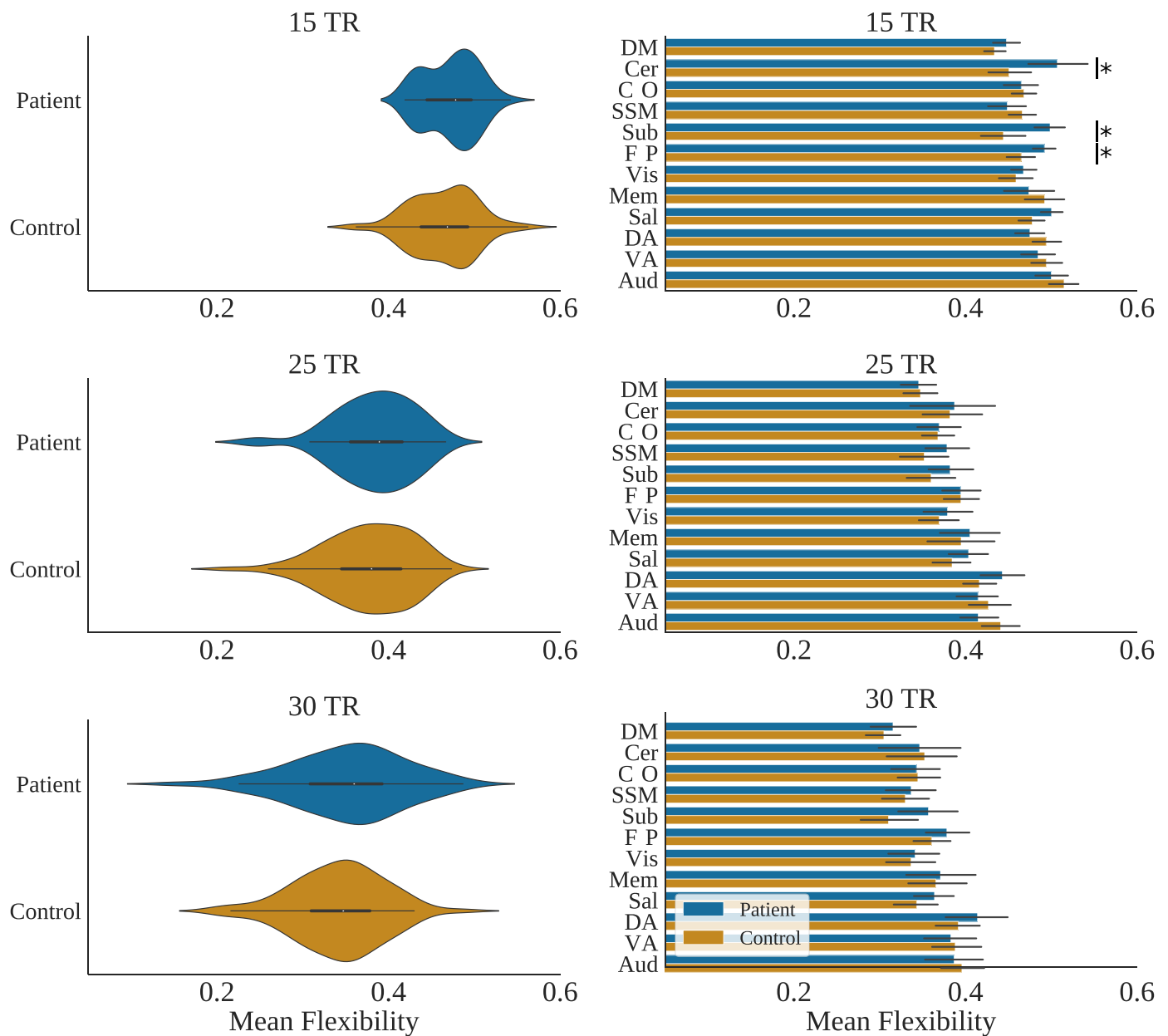


Fig. 5. Left column: Violin plots of whole brain (mean across nodes) flexibility for patients and controls for 15, 25, and 30 TR window sizes. Right column: mean flexibility values for patients with schizophrenia and controls averaged across resting state networks for each TR window size. Asterisks show $P < 0.05$ (FDR corrected) for group differences, whilst controlling for spike percentage.

Table. 3

Spearman's Rho correlations of PANSS scores (positive, and negative), medication use at time of scan (Olanzapine equivalent in mg), duration of psychotic illness, and age of onset of psychotic symptoms, with whole brain (15, 25, and 30 TR windows), resting state network (RSN), and node flexibility values, within the patient group. P values reported as uncorrected for multiple comparisons. Fronto-parietal TC = Fronto-parietal Task Control.

	PANSS Positive	P	PANSS Negative	P	Olanzapine Equivalent	P	Duration of Illness	P	Illness Onset	P
Whole Brain 15 TR	-0.27	0.042	0.09	0.495	0.02	0.886	-0.07	0.626	-0.17	0.230
Whole Brain 25 TR	-0.24	0.078	0.12	0.366	0.07	0.613	-0.26	0.054	-0.13	0.359
Whole Brain 30 TR	-0.06	0.658	0.01	0.915	0.16	0.242	0.00	0.990	-0.12	0.405
Left Thalamus	-0.13	0.351	0.00	0.986	0.05	0.702	-0.18	0.182	0.02	0.895
Right Crus I	0.02	0.891	0.02	0.864	0.07	0.600	-0.19	0.179	0.13	0.363
Cerebellar RSN	-0.10	0.481	-0.01	0.925	0.01	0.951	0.07	0.592	0.08	0.575
Fronto-Parietal TC RSN	-0.26	0.058	-0.01	0.940	-0.15	0.299	0.01	0.958	0.09	0.537
Subcortical RSN	-0.15	0.270	0.02	0.901	0.01	0.945	-0.30	0.025	-0.10	0.483

Table 4

Patient and control mean and standard deviation (SD) of between RSN synchronisation (BRSNS) scores for each pair of RSN found to have significantly different means after FDR correction. Table shows T tests with degrees of freedom (DOF), and FDR corrected P values.

Resting State Network Pairs	Patient Mean	Patient SD	Control Mean	Control SD	T	DOF	P (FDR)
SSM Salience	0.21	0.03	0.19	0.04	3.61	123.97	0.010
SSM Subcortical	0.21	0.05	0.18	0.06	3.51	123.72	0.010
DA Salience	0.24	0.04	0.21	0.05	2.77	119.49	0.047
DA Subcortical	0.21	0.05	0.18	0.05	3.35	118.74	0.014
Memory Cerebellar	0.18	0.07	0.27	0.10	-5.36	124.51	0.000
Memory Subcortical	0.21	0.06	0.25	0.11	-2.86	113.03	0.041
Auditory Cerebellar	0.27	0.08	0.23	0.07	2.93	102.14	0.039
Auditory Subcortical	0.30	0.06	0.26	0.07	3.22	122.99	0.018
Salience Subcortical	0.26	0.05	0.31	0.08	-4.26	119.93	0.001

left thalamus (MNI XYZ: -2, -13, 12), which was previously found to have significantly higher flexibility scores in the patient group (Fig. 7). This was done as the thalamus is known to be an important hub, mediating connections between subcortical, sensory-motor, and cortical regions (Hwang et al., 2017) and has particular importance in schizophrenia pathology (Andreassen et al., 1994; Anticevic et al., 2013; Bernard et al., 2015, 2017). Transition matrices were created for 15 TR windows only.

Statistical comparisons of group mean transition probabilities were made using permutation tests of group differences (two tailed; 5000 permutations of group assignments). There were no significant group differences in the probability of transition between any of the communities at the whole brain level. For the left thalamus, there was a significantly greater group mean probability of transition in patients between communities 1 and 4 (mean difference = 0.13, $p = 0.025$). Probability of transition between communities 1 and 4 in patients was not associated with PANSS positive ($r_s = 0.17$, $p = 0.201$) or negative ($r_s = 0.08$, $p = 0.582$) symptom scores, but was significantly positively correlated with duration of psychotic illness ($r_s = 0.29$, $p = 0.031$). When visualising cluster centres from the K mean clustering procedure, averaged within each RSN, it appeared that community 1 represented the default mode / memory retrieval networks and community 4 the sensory-somatomotor network (Fig. 7).

3.10. Confounding factors

Restricting results to right handed participants gave similar results in terms of group differences of flexibility scores at the whole brain and RSN level. At the node level, results were similar, however flexibility scores were suggested to be higher in patients for nodes in four additional regions: the left posterior cingulate gyrus (MNI: -2, -35, 31; $F(1124) = 12.40$, $p(\text{FDR}) < 0.001$), the right middle frontal gyrus (MNI: 31, 33, 26; $F(1124) = 13.30$, $p(\text{FDR}) < 0.001$), and the right thalamus (MNI: 6, -24, 0; $F(1124) = 11.15$, $p(\text{FDR}) = 0.001$).

Using overlapping time windowed correlation matrices (15 TR windows incrementing in 1 TR steps) resulted in non-significant results at the whole brain and RSN level. The left thalamus still appeared to have significantly higher flexibility scores in patients ($F(1124) = 15.24$, $p(\text{FDR}) < 0.001$). Flexibility scores from overlapping and non-overlapping windows at the whole brain level were however strongly correlated $R = 0.52$, $p < 0.001$ across participants.

The mean number of communities in time windows was not significantly different between the two groups ($t(97.60) = -0.24$, $p = 0.813$). It was also not correlated with flexibility scores in the cerebellar ($R = 0.01$, $p = 0.950$), fronto-parietal task control ($R = 0.05$, $p = 0.570$), or subcortical networks ($R = 0.10$, $p = 0.242$). Neither was it correlated with flexibility scores in the left thalamus ($R = 0.04$, $p = 0.632$). This suggests it did not act as a mediator for the relationship between group assignment and flexibility.

3.11. Association between mean correlation of time windows and flexibility

There were significant median group differences in the mean correlation across time windows (mean of each correlation matrix, averaged across time windows), suggesting control group time windows to have higher functional connectivity (patient median (IQR) = 0.19 (0.12), control median (IQR) = 0.27 (0.17); Mann Whitney $U = 2875$, $p < 0.001$). It was therefore tested whether mean time window correlation accounted for group differences in flexibility scores. To do so, a mediation analysis was carried out with flexibility score as the dependent variable (for nodes and RSNs found to be significantly different between groups), group assignment as the independent variable, and mean time window correlation as the mediator. It appeared that for all significant results the relationship between group assignment and flexibility score was accounted for by the mean of time window correlation matrices (supplementary materials Section 8).

4. Discussion

Higher flexibility (network community switching) scores in patients with schizophrenia has been suggested to show less organised and less stable network modular organisation in schizophrenia (Braun et al., 2016). The current study aimed to both confirm this finding and to explore novel methods to further describe alterations in dynamic modular structure. We found higher flexibility scores in participants with schizophrenia in cerebellar, subcortical, and fronto-parietal task control RSNs, as well as in an area of the left thalamus and right crus I (an area of the cerebellum). Such findings support the suggestions that schizophrenia involves altered brain network dynamics (Damaraju et al., 2014; Du et al., 2017; Sakoğlu et al., 2010) and extends the suggestion of disorganised and unstable network dynamics in schizophrenia to the brain at rest. The present study tested a range of methodological factors which appeared to impact results, highlighting a need for further exploration as to what measures such as flexibility represent.

In addition to the measure of flexibility, patterns of over and under 'between resting-state network synchronisation' suggested a complex pattern of over and under synchronisation of brain areas in patients with schizophrenia, highlighting the likely complexity of altered dynamic modular structure in schizophrenia. The current study also supports evidence of altered dynamic functional connectivity of the thalamus in schizophrenia (Damaraju et al., 2014), highlighting its importance in schizophrenia pathology (Woodward et al., 2012). This was further supported by a post-hoc analysis which used the frequency of transitions between community assignments of the left thalamus.

4.1. Flexibility in controls

Across nodes flexibility scores were moderately positively correlated with strength, suggesting that it was higher for well-connected nodes. Similar to previous studies, the relative flexibility scores within

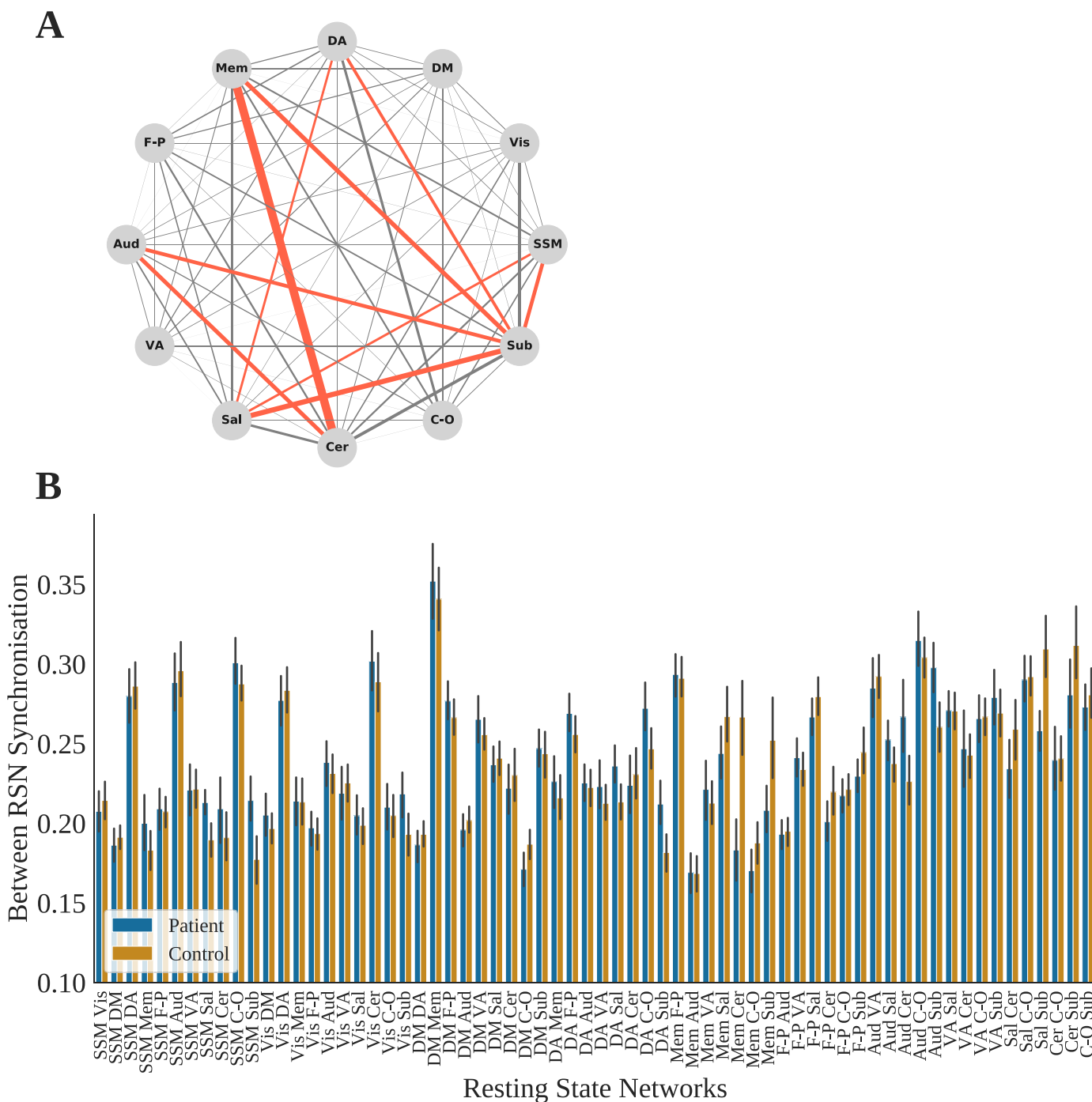


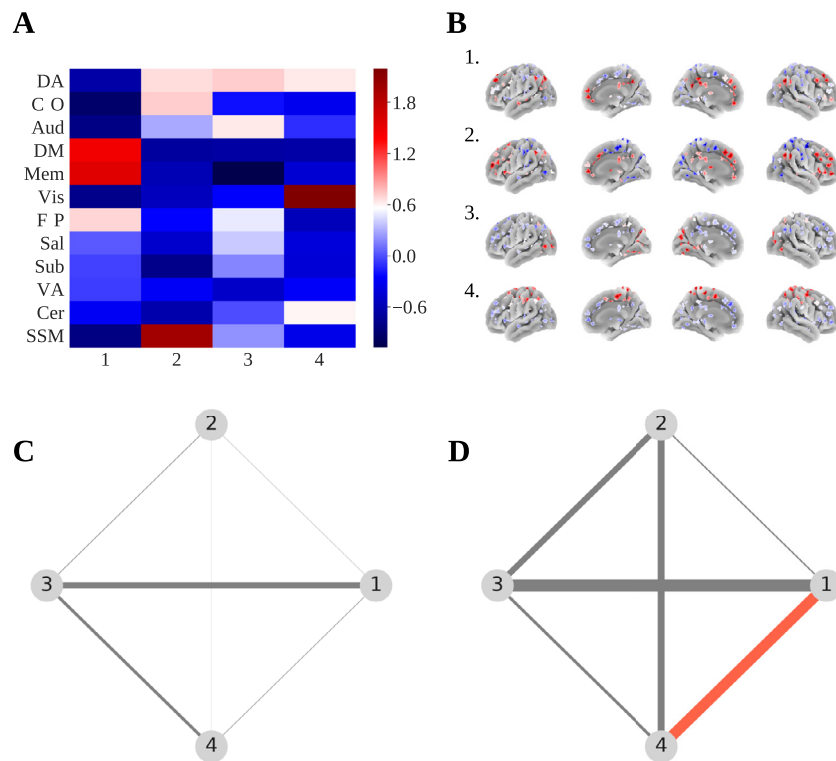
Fig. 6. (A) Network showing absolute group mean differences of between RSN synchronisation (BRSNS) scores, computed as the proportion of time two nodes share the same community averaged across nodes of each RSN pair. Red edges indicate p (FDR) < 0.05 group difference from an independent samples t test. (B) Control and schizophrenia group BRSNS scores for all RSN pairs. SSM = Sensory-SomatoMotor, DA = Dorsal Attention, VA = Ventral Attention, DM = Default Mode, FP = FrontoParietal task control, Aud = Auditory, Mem = Memory, Sub = Subcortical, Sal = salience, C-O = Cingulo-Opercular task control, Cer = Cerebellar. (For interpretation of the references to color in this figure legend, the reader is referred to the web version of this article.)

RSNs only partially followed the suggested control / processing connectivity profiles suggested by Power et al. (2011). The ORSNS measure however, followed the suggested attributes of the RSNs more closely, with the ‘processing’ systems (default mode, visual, sensory-somato-motor) (Power et al., 2011) typically having the lowest out of RSN synchronisation. This suggests some credibility for the module allegiance procedure used in the current study.

4.2. Group differences in flexibility

Significantly higher flexibility scores within the cerebellar, sub-cortical and salience networks suggested higher flexibility scores to be driven by community switching in these RSNs. This appears plausible given evidence of altered fronto-parietal RSN functional connectivity in schizophrenia (Chang et al., 2014; Rotarska-Jagiela et al., 2010; Sheffield et al., 2015; Skudlarski et al., 2010; Zhou et al., 2007), that the subcortical network contains areas involved in dopaminergic

Fig. 7. (A) Heatmap showing K means cluster centres averaged within each RSN and z score standardised. (B) Probability of node assignment to each clustered community centre projected onto a cortical surface. (C) Network showing the difference (patients – controls) of the probability of transition from one tokenised community to another for all brain areas. Size of edge represents edge weight. (D) Network showing the difference (patients – controls) of the probability of transition from one tokenised community to another for a node in the left thalamus found to have significantly different flexibility between groups (MNI XYZ: -2, -13, 12). Red colour indicates $p < 0.05$. (For interpretation of the references to color in this figure legend, the reader is referred to the web version of this article.)



pathways (Howes and Kapur, 2009), and given studies implicating the importance of the functional connectivity of the cerebellum in schizophrenia (Chen et al., 2013; Collin et al., 2011; Liu et al., 2011; Yu et al., 2013).

Higher flexibility scores in the patient group may suggest flexibility to represent a compensatory feature of brain dynamics in schizophrenia, which is supported by the tendency for flexibility to be higher during demanding cognitive tasks in healthy participants (Bassett et al., 2011; Pedersen et al., 2018; Telesford et al., 2016) and the “excess” of flexibility of participants with schizophrenia during a working memory task (Braun et al., 2016). Though the current study involved functional connectivity at rest, resting state functional connectivity is suggested to involve a constant reorganisation between ‘task negative’ and ‘task positive’ systems (Chai et al., 2012; Chang and Glover, 2010; Fox et al., 2005).

The inclusions of the subcortical and cerebellar networks in significant group differences of BRSNS suggests higher flexibility scores to be related to dynamic changes in the communication between RSN systems. The particular pattern of over and under synchronisation in the schizophrenia group suggests a complex time varying evolution of community structure which is altered in patients with schizophrenia. This is a novel finding that needs to be replicated in future studies.

4.3. Higher flexibility in the left thalamus

At the node level flexibility scores were significantly greater in a node covering the left thalamus. The thalamus is suggested to act as a major relay hub, regulating inputs from multiple brain areas, and may have a particular role in the pathophysiology of schizophrenia (Andreasen et al., 1994; Shenton et al., 2001). Disordered connectivity between the thalamus and other brain areas has been described in patients with schizophrenia (Anticevic et al., 2013; Klingner et al., 2014; Woodward et al., 2012) and those with prodromal symptoms (Anticevic

et al., 2015; Bernard et al., 2017).

When looking at the probability of transition between tokenised communities in patients with schizophrenia, the left thalamus was more likely to transition between a community representing the default mode network and a community mostly covering the sensory-somatomotor networks. This supports evidence of hyper-connectivity between the thalamus and sensory-motor areas in schizophrenia populations (Anticevic et al., 2013, 2015; Damaraju et al., 2014; Klingner et al., 2014). A study using the same freely available dataset also reported hyper-connectivity between the thalamus and sensorimotor brain areas (Chen et al., 2019).

4.4. Limitations

Though results were plausible and functional connectivity is suggested to be estimable from similarly sized time frames (Hutchison et al., 2013; Jones et al., 2012; Wilson et al., 2015), because fMRI data were only acquired for 5 minutes, there were relatively few time-points (150 volumes), which is not ideal for a dynamic functional connectivity analysis. Future studies may benefit from exploring methods that allow for a close to single time point resolution. These include Instantaneous Phase Synchrony (Glerean et al., 2012; Pedersen et al., 2018; Ponce-Alvarez et al., 2015) and Multiplication of Temporal Derivatives (Shine et al., 2015).

A number of other factors appeared to influence flexibility scores. The current study repeated group comparisons using another parcellation scheme (Gordon et al., 2016) and found this to affect results, suggesting that region of interest definition can have a problematic impact on findings (Smith et al., 2011). Results were also only significant at the RSN and node level for 15 TR windows, which may have been due to the smaller number of time windows when using larger window sizes. Future studies using larger datasets or longer / lower TR resting state scans may be better suited to analyses of this type. Using

overlapping windows appeared to reduce power of group comparisons, suggesting this to add no benefit over the use of non-overlapping windows. Varying multilayer community detection parameters as well as proportional cost thresholds of weighted adjacency matrices appeared to have unpredictable effects on group differences (supplementary material figure 1.2). The variability of results relating to methodological choices or “researcher degrees of freedom” (Simmons et al., 2011; Wicherts et al., 2016) suggests that care needs to be taken in interpreting measures derived from multilayer community detection. Group differences in flexibility and between RSN synchronisation also appeared to be dependent on differences in the mean correlation of windowed correlation matrices, suggesting that multilayer community assignment based measures may be no better than simpler network measures as simple biomarkers for schizophrenia.

Results in the present study were specific to a frequency range of 0.08–0.15 Hz. This may be problematic, as the influence of high frequency physiological noise is unknown. It is further complicated by the interaction between the window size used and the frequencies included. The suggested “rule of thumb” for the minimum window size (Leonardi and Van De Ville, 2015) suggests that a minimum window size of 100 s is appropriate for a typical band-pass of 0.01–0.1 Hz, which was not included in our study, in view of the limited number of time points. It is possible more typical frequency ranges such as 0.01–0.1 Hz could contain clinically useful information if studied with the current methodology, which warrants investigation in future studies with longer scanning sessions. A general limitation for analyses using sliding time windows is that there is no established ground truth for functional connectivity estimates, although several studies have used simulated data to explore the effects of frequency and window size (Leonardi and Van De Ville, 2015; Sakoğlu et al., 2010; Shakil et al., 2016).

4.5. Conclusions and future directions

Consistent with previous findings (Braun et al., 2016) the current study suggested flexibility (multilayer community switching) to be higher in patients with schizophrenia than controls. Data from the present study suggests that this may be driven by alterations in the dynamic modular configuration of subcortical, fronto-parietal task control, and cerebellar networks, and that the thalamus and right crus I area of the cerebellum may be of particular importance. This paper exhibits novel methods of BRNS and probability of transition between K means tokenised communities. Though these novel methods produced plausible results, they are presented as exploratory and as such need to be validated in further samples.

This paper highlights the impact of a range of methodological choices on results, such as window size, level of thresholding for graphs, and multilayer community detection resolution parameters. Despite methodological complexity, multilayer community detection offers unique time dependent ways of analysing fMRI data and allows for other measures not explored here, e.g. promiscuity (Papadopoulos et al., 2016). Future studies may benefit from exploring such alternative methods as well as the novel methods described in the current study.

CRediT authorship contribution statement

George Gifford: Conceptualization, Methodology, Software, Formal analysis, Validation, Writing - original draft, Writing - review & editing, Visualization. **Nicolas Crossley:** Conceptualization, Methodology, Supervision, Writing - review & editing. **Matthew J Kempton:** Supervision, Writing - review & editing. **Sarah Morgan:** Methodology, Software, Writing - review & editing. **Paola Dazzan:** Supervision, Writing - review & editing. **Jonathan Young:** Software. **Philip McGuire:** Conceptualization, Supervision, Writing - review & editing, Funding acquisition.

Declarations of Competing Interest

The authors declare no competing interests for the current study.

Acknowledgments

George Gifford is supported by the National Institute for Health Research (NIHR) Collaboration for Leadership in Applied Health Research and Care South London at King's College Hospital NHS Foundation Trust. The views expressed are those of the authors and not necessarily those of the NHS, the NIHR or the Department of Health.

The data (imaging and phenotypic) was collected and shared by the University of New Mexico funded by the National Institute of Health Centre of Biomedical Research Excellence (COBRE) grant 1P20RR021938-01A2 and the Mind Research Network.

This paper represents independent research part funded by the National Institute for Health Research (NIHR) Biomedical Research Centre at South London and Maudsley NHS Foundation Trust and King's College London. The views expressed are those of the authors and not necessarily those of the NHS, the NIHR or the Department of Health and Social Care.

Dr Nicolas Crossley is supported by the Comisión Nacional de Investigación Científica y Tecnológica: CONICYT FONDECYT regular 1160736 and CONICYT PIA ACT192064.

Dr Sarah Morgan holds a Henslow Fellowship at Lucy Cavendish College, University of Cambridge that is funded by the Cambridge Philosophical Society.

Supplementary materials

Supplementary material associated with this article can be found, in the online version, at doi:10.1016/j.nicl.2020.102169.

References

- Alexander-Bloch, A.F., Gogtay, N., Meunier, D., Birn, R., Clasen, L., Lalonde, F., ... Bullmore, E.T., 2010. Disrupted modularity and local connectivity of brain functional networks in childhood-onset schizophrenia. *Front. Syst. Neurosci.* 4, 147.
- Allen, E.A., Damaraju, E., Plis, S.M., Erhardt, E.B., Eichele, T., Calhoun, V.D., 2014. Tracking whole-brain connectivity dynamics in the resting state. *Cereb. Cortex* 24 (3), 663–676. <https://doi.org/10.1093/cercor/bhs352>.
- Andreasen, N.C., Arndt, S., Swayze, V., Cizadlo, T., Flaum, M., O'Leary, D., ... Yuh, W., 1994. Thalamic abnormalities in schizophrenia visualized through magnetic resonance image averaging. *Science* 266 (5183), 294–298.
- Anticevic, A., Cole, M.W., Repovs, G., Murray, J.D., Brumbaugh, M.S., Winkler, A.M., ... Glahn, D.C., 2013. Characterizing thalamo-cortical disturbances in schizophrenia and bipolar illness. *Cereb. Cortex* 24 (12), 3116–3130.
- Anticevic, A., Haut, K., Murray, J.D., Repovs, G., Yang, G.J., Diehl, C., ... Goodyear, B., 2015. Association of thalamic dysconnectivity and conversion to psychosis in youth and young adults at elevated clinical risk. *JAMA Psychiatry* 72 (9), 882–891.
- Bassett, D.S., Porter, M.A., Wymbs, N.F., Grafton, S.T., Carlson, J.M., Mucha, P.J., 2013. Robust detection of dynamic community structure in networks. *Chaos Interdiscip. J. Nonlinear Sci.* 23 (1), 013142.
- Bassett, D.S., Wymbs, N.F., Porter, M.A., Mucha, P.J., Carlson, J.M., Grafton, S.T., 2011. Dynamic reconfiguration of human brain networks during learning. *Proc. Natl. Acad. Sci.* 108 (18), 7641–7646.
- Bassett, D.S., Wymbs, N.F., Rombach, M.P., Porter, M.A., Mucha, P.J., Grafton, S.T., 2013. Task-based core-periphery organization of human brain dynamics. *PLoS Comput. Biol.* 9 (9), e1003171.
- Bassett, D.S., Yang, M., Wymbs, N.F., Grafton, S.T., 2015. Learning-induced autonomy of sensorimotor systems. *Nat. Neurosci.* 18 (5), 744.
- Bernard, J.A., Orr, J.M., Mittal, V.A., 2015. Abnormal hippocampal–thalamic white matter tract development and positive symptom course in individuals at ultra-high risk for psychosis. *NPJ Schizophr.* 1, 15009.
- Bernard, J.A., Orr, J.M., Mittal, V.A., 2017. Cerebello-thalamo-cortical networks predict positive symptom progression in individuals at ultra-high risk for psychosis. *NeuroImage Clin.* 14, 622–628.
- Betzler, R.F., Satterthwaite, T.D., Gold, J.I., Bassett, D.S., 2017. Positive affect, surprise, and fatigue are correlates of network flexibility. *Sci. Rep.* 7 (1), 520.
- Braun, U., Schäfer, A., Bassett, D.S., Rausch, F., Schweiger, J.I., Bilek, E., ... Geiger, L.S., 2016. Dynamic brain network reconfiguration as a potential schizophrenia genetic risk mechanism modulated by NMDA receptor function. *Proc. Natl. Acad. Sci.* 113 (44), 12568–12573.
- Braun, U., Schäfer, A., Walter, H., Erk, S., Romanczuk-Seiferth, N., Haddad, L., ... Tost, H., 2015. Dynamic reconfiguration of frontal brain networks during executive cognition

- in humans. *Proc. Natl. Acad. Sci.* 112 (37), 11678–11683.
- Chai, X.J., Castañón, A.N., Öngür, D., Whitfield-Gabrieli, S., 2012. Anticorrelations in resting state networks without global signal regression. *Neuroimage* 59 (2), 1420–1428.
- Chang, C., Glover, G.H., 2010. Time–frequency dynamics of resting-state brain connectivity measured with fMRI. *Neuroimage* 50 (1), 81–98.
- Chang, X., Shen, H., Wang, L., Liu, Z., Xin, W., Hu, D., Miao, D., 2014. Altered default mode and fronto-parietal network subsystems in patients with schizophrenia and their unaffected siblings. *Brain Res.* 87–99 1562.
- Chen, P., Ye, E., Jin, X., Zhu, Y., Wang, L., 2019. Association between Thalamocortical Functional Connectivity Abnormalities and Cognitive Deficits in Schizophrenia. *Sci. Rep.* 9 (1), 2952.
- Chen, T., Cai, W., Ryali, S., Supekar, K., Menon, V., 2016. Distinct global brain dynamics and spatiotemporal organization of the salience network. *PLoS Biol.* 14 (6), e1002469.
- Chen, Y.-L., Tu, P.-C., Lee, Y.-C., Chen, Y.-S., Li, C.-T., Su, T.-P., 2013. Resting-state fMRI mapping of cerebellar functional dysconnections involving multiple large-scale networks in patients with schizophrenia. *Schizophr. Res.* 149 (1–3), 26–34.
- Collin, G., Pol, H., Hilleke, E., Hajjima, S.V., Cahn, W., Kahn, R.S., van den Heuvel, M.P., 2011. Impaired cerebellar functional connectivity in schizophrenia patients and their healthy siblings. *Front. Psychiatry* 2, 73.
- Cox, R.W., 1996. AFNI: software for analysis and visualization of functional magnetic resonance neuroimages. *Comput. Biomed. Res.* 29 (3), 162–173.
- Damaraju, E., Allen, E.A., Belger, A., Ford, J.M., McEwen, S., Mathalon, D.H., ... Calhoun, V.D., 2014. Dynamic functional connectivity analysis reveals transient states of dysconnectivity in schizophrenia. *NeuroImage Clin.* 5, 298–308. <https://doi.org/10.1016/j.nicl.2014.07.003>.
- Deichmann, R., Gottfried, J.A., Hutton, C., Turner, R., 2003. Optimized EPI for fMRI studies of the orbitofrontal cortex. *Neuroimage* 19 (2), 430–441.
- Dong, D., Wang, Y., Chang, X., Luo, C., Yao, D., 2017. Dysfunction of large-scale brain networks in schizophrenia: a meta-analysis of resting-state functional connectivity. *Schizophr. Bull.* 44 (1), 168–181.
- Du, Y., Fryer, S.L., Fu, Z., Lin, D., Sui, J., Chen, J., ... Calhoun, V.D., 2018. Dynamic functional connectivity impairments in early schizophrenia and clinical high-risk for psychosis. *Brain Connectivity Dynamics* 180, 632–645. <https://doi.org/10.1016/j.neuroimage.2017.10.022>.
- Ellison-Wright, I., Bullmore, E., 2009. Meta-analysis of diffusion tensor imaging studies in schizophrenia. *Schizophr. Res.* 108 (1), 3–10.
- Fox, M.D., Snyder, A.Z., Vincent, J.L., Corbetta, M., Van Essen, D.C., Raichle, M.E., 2005. The human brain is intrinsically organized into dynamic, anticorrelated functional networks. *Proc. Natl. Acad. Sci.* 102 (27), 9673–9678.
- Glerean, E., Salmi, J., Lahnakoski, J.M., Jääskeläinen, I.P., Sams, M., 2012. Functional magnetic resonance imaging phase synchronization as a measure of dynamic functional connectivity. *Brain Connect.* 2 (2), 91–101.
- Gonzalez-Castillo, J., Hoy, C., Handwerker, D., Robinson, M., & Bandettini, P. (2013). Detection of Consistent Cognitive Processing at the Single Subject Level Using Whole-Brain fMRI Connectivity. Presentation at Soc Neurosci, San Diego (CA).
- Gordon, E., Laumann, T., Adeyemo, B., Huckins, J., Kelley, W., Petersen, S., 2016. Generation and Evaluation of a Cortical Area Parcellation from Resting-State Correlations. *Cereb. Cortex* 26 (1), 288–303 (New York, NY: 1991).
- Howes, O.D., Kapur, S., 2009. The dopamine hypothesis of schizophrenia: version III – the final common pathway. *Schizophr. Bull.* 35 (3), 549–562.
- Hutchinson, R.M., Womelsdorf, T., Gati, J.S., Everling, S., Menon, R.S., 2013. Resting-state networks show dynamic functional connectivity in awake humans and anesthetized macaques. *Hum. Brain Mapp.* 34 (9), 2154–2177.
- Hwang, K., Bertolero, M.A., Liu, W.B., D'Esposito, M., 2017. The human thalamus is an integrative hub for functional brain networks. *J. Neurosci.* 37 (23), 5594–5607.
- Jenkinson, M., Beckmann, C.F., Behrens, T.E.J., Woolrich, M.W., Smith, S.M., 2012. *Fsl Neuroimage* 62 (2), 782–790. <https://doi.org/10.1016/j.neuroimage.2011.09.015>.
- Jones, D.T., Vemuri, P., Murphy, M.C., Gunter, J.L., Senjem, M.L., Machulda, M.M., ... Knopman, D.S., 2012. Non-stationarity in the “resting brain’s” modular architecture. *PLoS One* 7 (6) e39731.
- Jutla, I. S., Jeub, L. G. S., & Mucha, P. J. (2011). A generalized Louvain method for community detection implemented in MATLAB. URL <http://Netwiki. Amath. Unc. Edu/GenLouvain>.
- Klingner, C.M., Langbein, K., Dietzek, M., Smesny, S., Witte, O.W., Sauer, H., Nenadic, I., 2014. Thalamocortical connectivity during resting state in schizophrenia. *Eur. Arch. Psychiatry Clin. Neurosci.* 264 (2), 111–119.
- Kühn, S., Gallinat, J., 2011. Resting-state brain activity in schizophrenia and major depression: a quantitative meta-analysis. *Schizophr. Bull.* 39 (2), 358–365.
- Leonardi, N., Van De Ville, D., 2015. On spurious and real fluctuations of dynamic functional connectivity during rest. *Neuroimage* 104, 430–436.
- Lerman-Sinkoff, D.B., Barch, D.M., 2016. Network community structure alterations in adult schizophrenia: identification and localization of alterations. *NeuroImage Clin.* 10, 96–106.
- Liu, H., Fan, G., Xu, K., Wang, F., 2011. Changes in cerebellar functional connectivity and anatomical connectivity in schizophrenia: a combined resting-state functional MRI and diffusion tensor imaging study. *J. Magn. Reson. Imaging* 34 (6), 1430–1438.
- Lynall, M.-E., Bassett, D.S., Kerwin, R., McKenna, P.J., Kitzbichler, M., Muller, U., Bullmore, E., 2010. Functional connectivity and brain networks in schizophrenia. *J. Neurosci.* 30 (28), 9477–9487.
- Mucha, P.J., Richardson, T., Macon, K., Porter, M.A., Onnela, J.-P., 2010. Community structure in time-dependent, multiscale, and multiplex networks. *Science* 328 (5980), 876–878.
- Newman, M.E., Girvan, M., 2004. Finding and evaluating community structure in networks. *Phys. Rev. E* 69 (2), 026113.
- Newman, M.E.J., 2006. Modularity and community structure in networks. *Proc. Natl. Acad. Sci.* 103 (23), 8577–8582.
- O'Neill, A., Mechelli, A., Bhattacharyya, S., 2018. Dysconnectivity of large-scale functional networks in early psychosis: a meta-analysis. *Schizophr. Bull.*
- Papadopoulos, L., Puckett, J.G., Daniels, K.E., Bassett, D.S., 2016. Evolution of network architecture in a granular material under compression. *Phys. Rev. E* 94 (3), 032908.
- Patel, A.X., Kundu, P., Rubinov, M., Jones, P.S., Vértes, P.E., Ersche, K.D., ... Bullmore, E.T., 2014. A wavelet method for modeling and despiking motion artifacts from resting-state fMRI time series. *Neuroimage* 95, 287–304.
- Pedersen, M., Omidvarnia, A., Zalesky, A., Jackson, G.D., 2018. On the relationship between instantaneous phase synchrony and correlation-based sliding windows for time-resolved fMRI connectivity analysis. *Neuroimage* 181, 85–94.
- Pedersen, M., Zalesky, A., Omidvarnia, A., Jackson, G.D., 2018. Multilayer network switching rate predicts brain performance. *Proc. Natl. Acad. Sci.* 115 (52), 13376–13381.
- Pedregosa, F., Varoquaux, G., Gramfort, A., Michel, V., Thirion, B., Grisel, O., ... Dubourg, V., 2011. Scikit-learn: machine learning in python. *J. Mach. Learn. Res.* 12 (Oct), 2825–2830.
- Pettersson-Yeo, W., Allen, P., Benetti, S., McGuire, P., Mechelli, A., 2011. Dysconnectivity in schizophrenia: where are we now. *Neurosci. Biobehav. Rev.* 35 (5), 1110–1124. <https://doi.org/10.1016/j.neubiorev.2010.11.004>.
- Ponce-Alvarez, A., Deco, G., Hagmann, P., Romani, G.L., Mantini, D., Corbetta, M., 2015. Resting-state temporal synchronization networks emerge from connectivity topology and heterogeneity. *PLoS Comput. Biol.* 11 (2), e1004100.
- Power, J.L., Cohen, A.L., Nelson, S.M., Wig, G.S., Barnes, K.A., Church, J.A., ... Schlaggar, B.L., 2011. Functional network organization of the human brain. *Neuron* 72 (4), 665–678.
- Rashid, B., Arbabshirani, M.R., Damaraju, E., Cetin, M.S., Miller, R., Pearlson, G.D., Calhoun, V.D., 2016. Classification of schizophrenia and bipolar patients using static and dynamic resting-state fMRI brain connectivity. *Neuroimage* 134, 645–657.
- Rashid, B., Damaraju, E., Pearlson, G.D., Calhoun, V.D., 2014. Dynamic connectivity states estimated from resting fMRI Identify differences among Schizophrenia, bipolar disorder, and healthy control subjects. *Front. Hum. Neurosci.* 8, 897. <https://doi.org/10.3389/fnhum.2014.00897>.
- Rotarska-Jagiela, A., van de Ven, V., Oertel-Knöchel, V., Uhlhaas, P.J., Vogeley, K., Linden, D.E., 2010. Resting-state functional network correlates of psychotic symptoms in schizophrenia. *Schizophr. Res.* 117 (1), 21–30.
- Sakoğlu, Ü., Pearlson, G.D., Kiehl, K.A., Wang, Y.M., Michael, A.M., Calhoun, V.D., 2010. A method for evaluating dynamic functional network connectivity and task-modulation: application to schizophrenia. *Magn. Reson. Mater. Phys. Biol. Med.* 23 (5–6), 351–366.
- Shakil, S., Lee, C.H., Keilholz, S.D., 2016. Evaluation of sliding window performance for characterizing dynamic functional connectivity and brain states. *Neuroimage* 133, 111–128. <https://doi.org/10.1016/j.neuroimage.2016.02.074>.
- Sheffield, J.M., Repovs, G., Harms, M.P., Carter, C.S., Gold, J.M., MacDonald III, A.W., ... Barch, D.M., 2015. Fronto-parietal and cingulo-opercular network integrity and cognition in health and schizophrenia. *Neuropsychologia* 73, 82–93.
- Shenton, M.E., Dickey, C.C., Frumin, M., McCarley, R.W., 2001. A review of MRI findings in schizophrenia. *Schizophr. Res.* 49 (1–2), 1–52.
- Shine, J.M., Koyejo, O., Bell, P.T., Gorgolewski, K.J., Gilat, M., Poldrack, R.A., 2015. Estimation of dynamic functional connectivity using multiplication of temporal derivatives. *Neuroimage* 122, 399–407.
- Shine, J.M., Koyejo, O., Poldrack, R.A., 2016. Temporal metastates are associated with differential patterns of time-resolved connectivity, network topology, and attention. *Proc. Natl. Acad. Sci.* 113 (35), 9888–9891.
- Shirer, W.R., Ryali, S., Rykhlevskaia, E., Menon, V., Greicius, M.D., 2012. Decoding subject-driven cognitive states with whole-brain connectivity patterns. *Cereb. Cortex* 22 (1), 158–165.
- Simmons, J.P., Nelson, L.D., Simonsohn, U., 2011. False-positive psychology: Undisclosed flexibility in data collection and analysis allows presenting anything as significant. *Psychol. Sci.* 22 (11), 1359–1366.
- Skudlarski, P., Jagannathan, K., Anderson, K., Stevens, M.C., Calhoun, V.D., Skudlarska, B.A., Pearlson, G., 2010. Brain connectivity is not only lower but different in schizophrenia: a combined anatomical and functional approach. *Biol. Psychiatry* 68 (1), 61–69.
- Smith, S.M., Miller, K.L., Salimi-Khorshidi, G., Webster, M., Beckmann, C.F., Nichols, T.E., ... Woolrich, M.W., 2011. Network modelling methods for FMRI. *Neuroimage* 54 (2), 875–891.
- Telesford, Q.K., Ashourvan, A., Wymbs, N.F., Grafton, S.T., Vettel, J.M., Bassett, D.S., 2017. Cohesive network reconfiguration accompanies extended training. *Hum. Brain Mapp.* 38 (9), 4744–4759.
- Telesford, Q.K., Lynall, M.-E., Vettel, J., Miller, M.B., Grafton, S.T., Bassett, D.S., 2016. Detection of functional brain network reconfiguration during task-driven cognitive states. *Neuroimage* 142, 198–210.
- Wicherts, J.M., Veldkamp, C.L., Augusteijn, H.E., Bakker, M., Van Aert, R., Van Assen, M.A., 2016. Degrees of freedom in planning, running, analyzing, and reporting psychological studies: a checklist to avoid p-hacking. *Front. Psychol.* 7, 1832.
- Wilson, R.S., Mayhew, S.D., Rollings, D.T., Goldstone, A., Przezdziak, I., Arvanitis, T.N., Bagshaw, A.P., 2015. Influence of epoch length on measurement of dynamic functional connectivity in wakefulness and behavioural validation in sleep. *Neuroimage* 112, 169–179.
- Woodward, N.D., Karbasforoushan, H., Heckers, S., 2012. Thalamocortical dysconnectivity in schizophrenia. *Am. J. Psychiatry* 169 (10), 1092–1099.
- Yu, Q., Plis, S.M., Erhardt, E.B., Allen, E.A., Sui, J., Kiehl, K.A., ... Calhoun, V.D., 2012. Modular organization of functional network connectivity in healthy controls and patients with schizophrenia during the resting state. *Front. Syst. Neurosci.* 5, 103.

Yu, Y., Shen, H., Zeng, L.-L., Ma, Q., Hu, D., 2013. Convergent and divergent functional connectivity patterns in schizophrenia and depression. *PLoS One* 8 (7), e68250.

Zheng, H., Li, F., Bo, Q., Li, X., Yao, L., Yao, Z., ... Wu, X., 2018. The dynamic characteristics of the anterior cingulate cortex in resting-state fMRI of patients with depression. *J. Affect. Disord.* 227, 391–397.

Zhou, Y., Liang, M., Jiang, T., Tian, L., Liu, Y., Liu, Z., ... Kuang, F., 2007. Functional dysconnectivity of the dorsolateral prefrontal cortex in first-episode schizophrenia using resting-state fMRI. *Neurosci. Lett.* 417 (3), 297–302.